

# A study of the photoneutron dose equivalent resulting from a Saturne 20 medical linac using Monte Carlo method

Seyed M. Hashemi,  
Bijan Hashemi-Malayeri,  
Gholamreza Raisali,  
Parvaneh Shokrani,  
Ali A. Sharafi

**Abstract.** High energy linacs have several advantages including lower skin dose and higher dose rate at deep sighted tumors. But, at higher energies photonuclear reactions produce neutron contamination. Photoneutron contamination has been investigated from the early days of modern linacs. However, more studies have become possible using Monte Carlo codes developed in recent years. The aim of this study was to investigate the photoneutron spectrum and dose equivalent produced by an 18 MV Saturne linac at different points of a treatment room and its maze. The MCNP4C code was used to simulate the transport of photoneutrons produced by a typical 18 MV Saturne linac. The treatment room of a radiotherapy facility in which a Saturne 20 linac is installed was modeled. Neutron dose equivalent was calculated and its variations at various distances from the center of the X-ray beam was studied. It was noted that by increasing the distance from the center of the beam, fast neutrons decrease rapidly, but thermal neutrons do not change significantly. In addition, the photoneutron dose equivalent was lower for smaller fields. The fast photoneutrons were not recorded in the maze. It can be concluded that the fast photoneutrons are highly attenuated by concrete barrier, while the slow photoneutrons are increased. In addition, increasing the X-ray field size increases the photoneutron dose equivalent around the treatment room and maze. It seems that the walls play an effective role in increasing the photoneutron dose equivalent.

**Key words:** photoneutron • linac • Monte Carlo method • MCNP4C • dose equivalent

S. M. Hashemi, B. Hashemi-Malayeri<sup>✉</sup>  
Department of Medical Physics,  
Tarbiat Modares University,  
P. O. Box 14115-151, Tehran, Iran,  
Tel.: +98 21 88011001, Fax: +98 21 88006544,  
E-mail: bijanhashemi@yahoo.com

G. Raisali  
Gamma Irradiation Center,  
Atomic Energy Organization of Iran,  
End of Kargare Shomali,  
P. O. Box 11365-3486, Tehran, Iran

P. Shokrani  
Department of Medical Physics and Engineering,  
Esfahan University of Medical Sciences,  
Hezarjarib, Esfahan, Iran

A. A. Sharafi  
Department of Radiology Technology,  
School of Paramedicine,  
Iran University of Medical Sciences,  
Hemmat highway, Tehran, Iran

Received: 19 June 2006  
Accepted: 2 January 2007

## Introduction

High-energy X-rays offer several advantages over lower energy photons including: lower skin dose, higher depth dose, smaller scattered dose to tissues outside the target volume and less rounded isodose curves. These advantages in physical dose distributions have led to significant improvements in clinical radiotherapy, and high energy linear accelerators are now a standard fixture of radiotherapy clinics. However, high-energy X-ray machines present a significant radiation protection problem by producing small amounts of neutrons. Neutrons can be produced by a photonuclear reaction. The total neutrons produced are composed of two parts: photonuclear reactions via bremsstrahlung, and electron production via virtual photons. In general, the cross sections of electron production interaction are expected to be of the order of the fine structure constant ( $\alpha \approx 1/137$ ) times of the cross sections of photonuclear reactions [11]. High energy photons generate neutrons through interactions with accelerator structures and treatment rooms [5]. Photonuclear absorption cross section for low atomic number materials such as O, C, and N is about a millibarn, but for high atomic number

materials like W, and Pb it is about 400 millibarns [4]. At the isocenter, the fluence  $\Phi$  ( $\text{n}\cdot\text{cm}^{-2}$ ) of photoneutron production per unit X-ray dose is as follows [8]:

$$(1) \quad \Phi_{tot} = \Phi_{sc} + \Phi_{th} + \Phi_{dir} = \frac{aQ}{4\pi d^2} + \frac{5.4aQ}{S} + \frac{1.26Q}{S}$$

where:  $\Phi_{dir}$  is the direct neutron fluence;  $\Phi_{sc}$  the scatter neutron fluence;  $\Phi_{th}$  the thermal neutron fluence;  $Q$  the neutron source strength per Gy-X-ray of the linac;  $a$  the transmission factor for the linac head (1 for Pb, and 0.85 for W);  $d$  the distance (cm) between the measurement point and the target;  $S$  the area of the treatment room ( $\text{cm}^2$ ). The  $Q$  value varies for different linacs including Varian series, Philips series, GE series [8]. It is claimed that the  $Q$  values are not significantly changed among various models of accelerators from the same manufacturer for a given energy [8]. However, this value changes significantly among accelerators from different manufacturers [8].

Evaporative photoneutrons create the peak of photoneutron spectra, while the tail of the spectra at higher energies is related to direct photoneutrons. An investigation has shown that the mean quality factor of photoneutron spectra is about 9.8 and 11.6 in and out of the X-ray field, respectively [6]. So, photoneutron dose equivalent could be high enough to induce new tumors and/or make some injuries. Since lead and other heavy materials are transparent to neutrons, it has been recommended to shield fetus and sensitive organs [6]. Another investigation on a Saturne 20 linac, using polycarbonate sheets through electrochemical etching (ECE), has reported a value about 3.3 mSv/Gy as the dose equivalent at the center of the  $40 \times 40 \text{ cm}^2$  field size of this linac [12]. In this study the shape of photoneutron spectrum is considered to be simply the same as the shape of a fission spectrum. Some measurements with bobble detectors on this linac have shown that the photoneutron dose equivalent in the water phantom is about 4.5 mSv/Gy [6]. For these measurements, the detectors are chosen in a way to cover completely the photoneutron spectrum [6]. In some other studies, the photoneutron spectrum has carefully been calculated, but the photoneutron dose equivalent has not been investigated [7]. In this work we have studied the photoneutron spectrum of a Saturne 20 (CGR) linac by simulating a simplified geometry and calculated its relevant dose equivalent in its treatment room and maze.

## Methods and materials

This study was carried out on a Saturne 20 (CGR) linear accelerator working at high energy (18 MV) and installed in a concrete treatment room having a six meter length maze with a lead door at Omid Hospital of Esfahan city in Iran (Fig. 1).

The photoneutrons produced in such high energy linacs are classified in two groups: one group having a Maxwellian energy distribution being called evaporative neutrons, and the other group being composed of direct

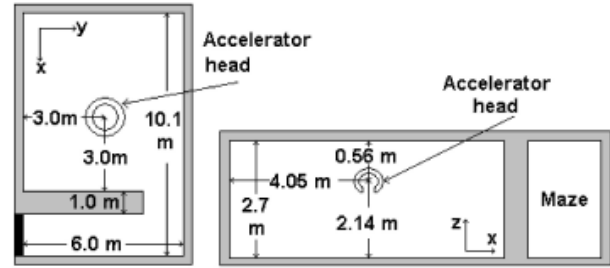


**Fig. 1.** The geometry of the concrete room in which the 18 MV Saturne linac is installed.

neutrons which are produced through direct interaction between high energy photons and the neutrons of the nucleus of target atoms. The evaporative neutrons constitute the largest number of photoneutrons whose spectra can be determined by the following equation [11]:

$$(2) \quad \frac{dN}{dE_n} = \frac{E_n}{T^2} \exp\left(\frac{-E_n}{T}\right)$$

in which  $E_n$  is the neutron energy in MeV and  $T$  is the “nuclear temperature” expressed in MeV that is assumed to be 0.5 MeV for W targets [11].

In order to evaluate the relative contribution of the distinct components of the total spectra, an isotropic neutron source was considered with an energy spectrum derived from the following equation [13]:

$$(3) \quad \frac{dN}{dE_n} = \frac{0.89E_n}{(0.5)^2} \exp\left(\frac{-E_n}{0.5}\right) + \frac{0.11 \ln\left[\frac{E_{max}}{E_n + 7.34}\right]}{\int_0^{E_{max}-7.34} \ln\left[\frac{E_{max}}{E_n + 7.34}\right] dE_n}$$

in which  $E_n$  is the neutron energy and  $E_{max}$  is the maximum energy of X-ray photon. So, when the X-ray energy is considered to be 18 MeV ( $E_{max}$ ), the photoneutron emission spectrum can be derived from the following equation:

$$(4) \quad \frac{dN}{dE_n} = 3.571E_n \cdot \exp(-2E_n) + 0.0261858 \ln\left(\frac{18}{E_n + 7.34}\right)$$

In this study, the MCNP4C Monte Carlo code, and the Evaluated Nuclear Data File B-VI (ENDF/B-VI) of continuous energy of neutron cross section library [2] was used to perform the simulations of photoneutrons transport. For the simulations, the source term was considered as an isotropic point-like spectrum given by Eq. (2). The accelerator head was modeled as a 10 cm tungsten sphere around the source where neutrons are produced in the same way reported by other authors [3, 7, 8]. In order to simulate different field sizes,

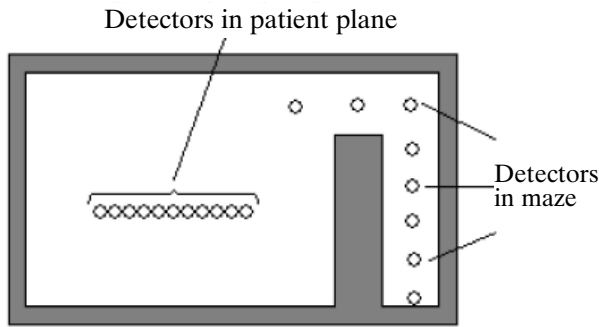


**Fig. 2.** The geometry of the simulation of the concrete room. The detectors are shown as placed in the treatment room and maze.

a variable aperture was defined in the wall of tungsten sphere providing various diameters.

In this study, the  $F_4$  tally of the MCNP4C code was used which calculates the mean fluence of particles in a volume cell using the distance traveled (track length) by the particles in the volume of interest. Indeed, the code calculates the mean of the fluence of particles being equal to the following integral:

$$(5) \quad F_4 = \iiint_{V,t,E} \Phi(\vec{r}, E, t) dEdT \cdot \frac{dV}{V}$$

Via this equation we can have:

$$(6) \quad F_4 = Tl/V$$

In these equations,  $\Phi(r, E, t)$  is the fluence of a particle with an energy of  $E$  which at the time of  $t$  reaches the position  $r$  and  $Tl$  is the total length traveled by the particle in the volume of the cell being presented by  $V$ .

Detectors were described and defined by spherical volumes with a diameter of 20 cm. The spheres were considered to be at a height of 114 cm from the floor for both of the treatment room and maze sites (Fig. 2). The concrete barrier was considered to have a density of 2.26 g/cm<sup>3</sup>, and constituted of 0.92% hydrogen, 49.83% oxygen, 1.71% sodium, 4.56% aluminum, 31.58% silicon, 1.92% potassium, 8.26% calcium and 1.22% iron (in terms of their weight percentage in the composition) [10]. To reduce the computation time, the thickness of the walls, ceiling and floor were all modeled to be 30 cm, instead of their real values. This was due to the negligible contribution of neutrons covering forward and backward distances larger than 30 cm [1]. This simplification was not used for the wall located between the treatment room and the maze. The entrance door was considered to be made of pure lead. In one of the simulation programs, the walls were not modeled at all, to be able to compare the effect of the walls. The simulation programs were carried out for 200 million particles. It is stated that the  $Q$  values are not significantly different among different models of accelerators from the same manufacturer for the same energy [8]. Therefore, we used the  $Q$  value reported for the Saturne 43, being 4E+12 neutrons per 1 Gy X-ray at the isocenter to calculate the dose equivalent

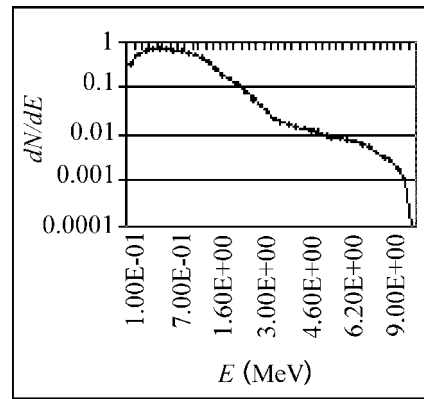


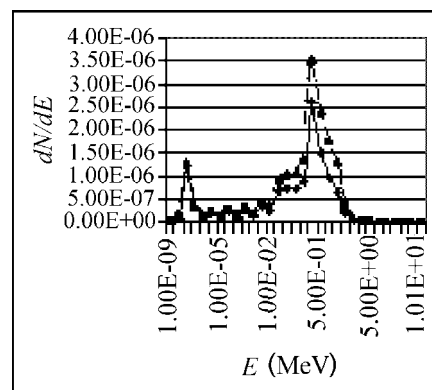
**Fig. 3.** The neutron spectra generated by an 18 MV linear accelerator, before the transport through its head (source spectrum).

from photoneutrons [8]. To calculate the neutron dose equivalent, neutron Flux-to-Dose Rate Conversion Factors as reported by the NCRP-38 [9] were used. To verify the results of our simulations, they were compared with the results of measurements reported by other authors [12].

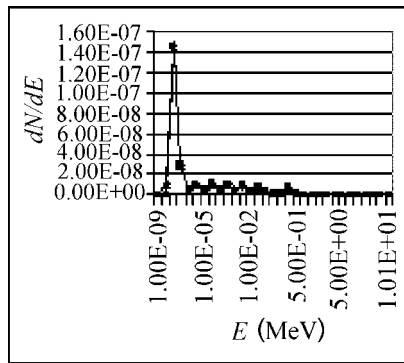
## Results

Figure 3 shows the neutron source spectra obtained from Eq. (3), for the Saturne 20 linac (at 18 MV) in this study, which was then used as the input for the simulation. As can be noted from the figure, the neutron emission spectra shows a predominance of neutrons with energies up to 2 MeV and a most probable energy about 0.5 MeV (due to the evaporation term). The neutron spectra produced by linear accelerators are slowed down in energy as a result of the particle interaction with the accelerator structures.

Results of our simulation have been shown in Figs. 4–10. Investigating photoneutron spectra reveals that increasing the therapeutic field size will increase the fluence of photoneutrons for all energies, although this is more obvious for the neutrons with higher energies (Fig. 4). The results also indicate that increasing the field dimensions dose not affect the thermal neutron



**Fig. 4.** Photoneutron spectra at the center of three different field sizes: 40 × 40 cm<sup>2</sup> (solid line), 25 × 25 cm<sup>2</sup> (dashed line), and 10 × 10 cm<sup>2</sup> (dotted line). Increasing the field size increases the fluence of high energy neutrons significantly.



**Fig. 5.** Photoneutron spectra at the midpoint of the maze. The peak of fast neutrons is absent and different field sizes:  $40 \times 40 \text{ cm}^2$  (solid line),  $25 \times 25 \text{ cm}^2$  (dashed line), and  $10 \times 10 \text{ cm}^2$  (dotted line) do not affect thermal neutrons.

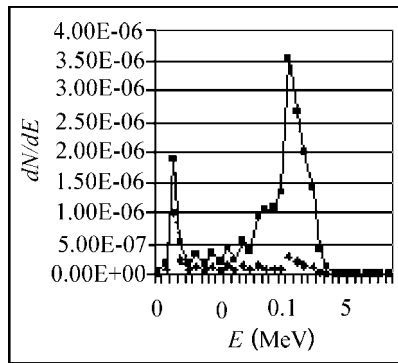


**Fig. 6.** Comparing photoneutron spectra at the center of X-ray field (solid line) and near the walls (dashed line).

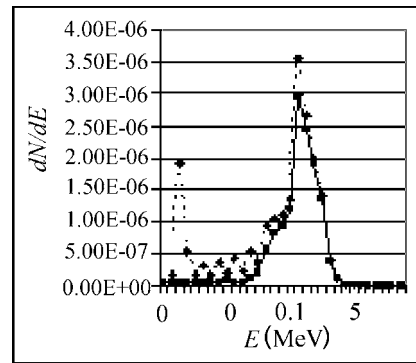


**Fig. 7.** Comparing photoneutron spectra with (solid line) and without the walls (dashed line).

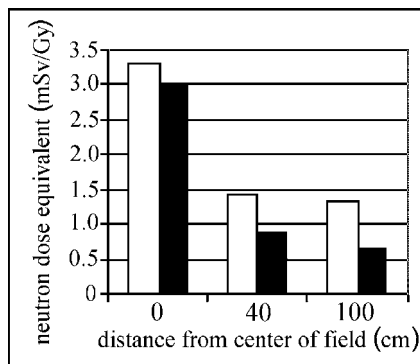


**Fig. 8.** Photoneutron dose equivalent is significantly higher due to the presence of the walls in the treatment room. With (white) and without the room (black).

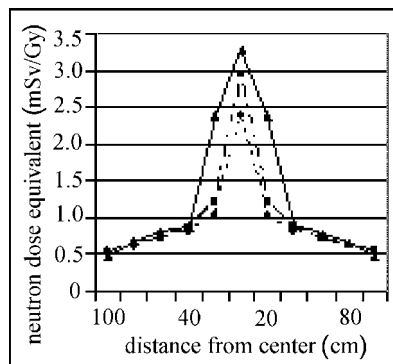


**Fig. 9.** Photoneutron dose equivalent in the treatment room for three field sizes:  $40 \times 40 \text{ cm}^2$  (solid line),  $25 \times 25 \text{ cm}^2$  (dashed line),  $10 \times 10 \text{ cm}^2$  (dotted line).

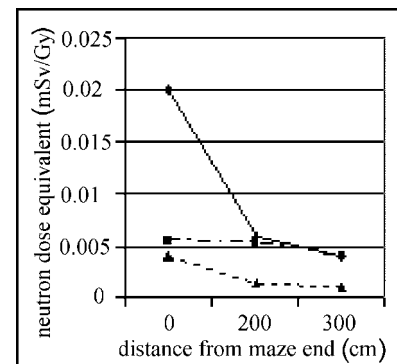


**Fig. 10.** Photoneutron dose equivalent in the maze for three field sizes:  $40 \times 40 \text{ cm}^2$  (solid line),  $25 \times 25 \text{ cm}^2$  (dashed line),  $10 \times 10 \text{ cm}^2$  (dotted line).

fluence, especially in the maze (Fig. 5). In addition, at larger distances, from the center of the X-ray field, it is noted that the fast neutron fluence decreases, while the thermal neutron fluence dose not change significantly (Fig. 6). An important point noted in this study was the absence of the thermal neutron peak in the spectrum when the walls of the treatment room were not considered in the simulation (Fig. 7). Results of simulations show that the walls of the treatment room results in a higher photoneutron dose equivalent at different points (Fig. 8). In general, this study shows that the dose equivalent of photoneutrons at the center of the X-ray field is a maximum, being about 3.3 mSv/Gy for a  $40 \times 40 \text{ cm}^2$  field size being in good agreement with the measurement results (Table 1). It was noted that by increasing the distance from the center of the field, the dose equivalent decreases gradually and reaches 0.5 mSv/Gy at a point 100 cm away from the center (Fig. 9).

Decreasing the field size results in obvious reduction in the dose equivalent of photoneutrons. As shown in Fig. 9, this parameter decreases from 3.3 mSv/Gy (for the  $40 \times 40 \text{ cm}^2$  field size) to 2.5 mSv/Gy (for the  $10 \times 10 \text{ cm}^2$  field size) having good agreement with the measurement results (Table 1).

In the maze, at points closer to the door, the dose equivalent of photoneutrons was lower. For example, at the entrance of the maze, the photoneutron dose equivalent was about 0.02 mSv/Gy, and reached  $5.5 \mu\text{Sv/Gy}$  at the midpoint of the maze and finally it became about  $4 \mu\text{Sv/Gy}$  for the  $40 \times 40 \text{ cm}^2$  field size near the door (Fig. 10). As shown in Fig. 10, decreasing the field size reduces the thermal neutron dose equivalent. In the midpoint of the maze the thermal neutron dose was 5.5, 5 and  $1 \mu\text{Sv/Gy}$  for the field sizes of  $40 \times 40$ ,  $25 \times 25$  and  $10 \times 10 \text{ cm}^2$ , respectively.

It can be claimed that the intensity and energy of fast neutrons (100 keV – 10 MeV) are attenuated due

**Table 1.** Comparison of the photoneutron dose equivalent (mSv/Gy X-ray) at tow points, between this study and that reported by Sohrabi *et al.* [12]

Distance from center of field (cm)	This work		Ref. [12]	
	0	20	0	20
$10 \times 10 \text{ cm}^2$	2.5	1.0	2.2	0.5
$25 \times 25 \text{ cm}^2$	2.9	1.2	3.0	1.3
$40 \times 40 \text{ cm}^2$	3.3	2.4	3.7	2.0

to scattering resulted from their interactions with the atoms of concrete material. The slowing down process leads to the generation of epithermal (1 eV – 100 keV) and thermal (1 meV – 1 eV) neutron fluxes.

## Conclusion

The undesired neutrons produced in medical linear accelerators are high energy neutrons whose energy distributions can be described by Eq. (2). According to Fig. 2, it can be seen that the rapid component of the spectrum is highly attenuated by the concrete barrier, increasing the thermal and epithermal neutrons. Increasing the X-ray field size increases the photoneutron dose equivalent in the treatment room and maze. Considering relatively high uncertainty existed in neutron dosimetry, this finding is in good agreement with the results reported by other authors [6, 12]. However, our results have a better agreement with one of the reports [12]. This may be due to the fact that these two studies have been carried out on the same machine with the same treatment room. The results show that in the maze the fast photoneutrons are absent which can be attributed to the moderating role of the concrete walls. Besides, the walls play an effective role in increasing the photoneutron dose equivalent at the patient plane. This may be due to the reflection of photoneutrons from the walls, and is in good agreement with other studies [1]. The method developed in this study can be used for calculating the photoneutron dose equivalent in radiotherapy facilities.

## References

1. Agosteo S, Foglio PA, Maggioni SV, Terrani S, Borasi G (1995) Radiation transport in a radiotherapy room. *Health Phys* 68:27–34
2. Briesmeister JF (2000) Manual of MCNP-4C™ – a general Monte Carlo n-particle transport code. Los Alamos, New Mexico
3. Carinou E, Kamenopoulou V (1999) Evaluation of neutron dose in the maze of medical accelerators. *Med Phys* 26:2520–2525
4. Chibani O, Ma CM (2003) Photonuclear dose calculations for high-energy photon beams from Siemens and Varian linacs. *Med Phys* 30:1990–2000
5. d'Errico F, Luszik-Bhadra M, Nath R, Siebert BRL, Wolf U (2001) Depth dose-equivalent energies of photoneutrons generated by 6–18 MeV X-ray beams for radiotherapy. *Health Phys* 80;1:4–113
6. d'Errico F, Nath R, Tana L, Corzio G, Alberts WG (1997) In-phantom dosimetry and spectrometry of photoneutrons from an 18 MeV linear accelerator. *Med Phys* 25:1717–1724
7. Facur A, Falcao RC, Silva AX, Crispim VR, Vitorelli JC (2005) A study of neutron spectra from medical linear accelerators. *Appl Radiat Isot* 62:69–72
8. Followill DS, Stoval MS, Kry SF, Ibbott GS (2003) Neutron source strength measurements for Varian Siemens Elekta and General Electric linear accelerator. *J Appl Clin Med Phys* 4:189–194
9. NCRP (1971) Protection against neutron radiation. NCRP Report 38, Scientific Committee 4 on Heavy Particles. National Council on Radiation Protection and Measurements, Bethesda, MD, USA
10. NCRP (1976) Structural shielding design and evaluation for medical use of X-rays and gamma rays of energies up to 10 MeV. NCRP Report 49. National Council on Radiation Protection and Measurements, Bethesda, MD, USA
11. NCRP (1984) Neutron contamination from medical accelerators. NCRP Report 79. National Council on Radiation Protection and Measurements, Washington DC, USA
12. Sohrabi M, Mostofizadeh A (1999) Measurement of photoneutron dose in and out of high energy X-ray beam of a Saturne 20 medical linear accelerator by ECE polycarbonate detectors. *Radiat Meas* 31:479–482
13. Tosi G, Torresin A, Agosteo S *et al.* (1991) Neutron measurements around medical electron accelerators by active and passive detection techniques. *Med Phys* 18;1:54–60